

# **Few Layered Metallic 1T-MoS<sub>2</sub>/TiO<sub>2</sub> with Exposed (001) Facets: Two-Dimensional Nanocomposites for Enhanced Photocatalytic Activities**

*by HyukSu Han et. al.*

## **- Supporting Information -**

### **EXPERIMENTAL DETAILS FOR CHARACTERIZATION**

#### ***Microstructural Analysis***

Scanning electron microscopy (SEM, Hitachi S4800) and transmission electron microscopy (TEM, JEOL 2100) were utilized to investigate 2D nanostructured 1T-MoS<sub>2</sub>/TiO<sub>2</sub>(001) (MST) nanocomposites.

#### ***Phase and Compositional Analysis***

X-ray diffraction (XRD) patterns were measured for TiO<sub>2</sub>, MST, and MoS<sub>2</sub> samples using D/MAX-2500/PC (Rigaku) diffractometer with Cu K $\alpha$  radiation ( $\lambda=0.15418$  nm) at 40 kV and 100 mA. Raman spectroscopy was performed via a dispersive laser spectrophotometer (NRS-3100, JASCO) at room temperature with an excitation wavelength of 633 nm. X-ray photoelectron spectroscopy (XPS) spectra were recorded for the samples using VG ESCALAB 200i (Thermoscientific). XPS survey and high resolution scans were conducted with the pass energies of 100 eV and 20 eV, respectively.

#### ***Photoelectrochemical Analysis***

UV-Visible optical absorption spectra were collected with a V-699 (JASCO) spectrometer

with a reference of dry-pressed BaSO<sub>4</sub> disk. Time-resolved photoluminescence (PL) spectrum was measured using a spectrophotometer (F-7000, Hitachi). Fluorescence lifetime decays were measured using an inverted-type scanning confocal microscope (MicroTime-200, Picoquant) with a 20x objective. A single-mode pulsed diode laser (379 nm with a pulse width of ~200 ps and a laser power of ~20 uW) were used as an excitation source. A dichroic mirror (Z375RDC, AHF), a longpass filter (HQ405lp, AHF), a 75 μm pinhole, a band-pass filter (400±20 or 450±20 nm), and an avalanche photodiode detector (PDM series, MPD) were used to collect emissions from the samples. Time-correlated single-photon counting technique was used to obtain fluorescence decay curves, as a function of time with a resolution of 16 ps, during image scanning. Exponential fittings for the obtained fluorescence decays were performed by the iterative least-squares deconvolution fitting using the Symphotime software (version 5.3).

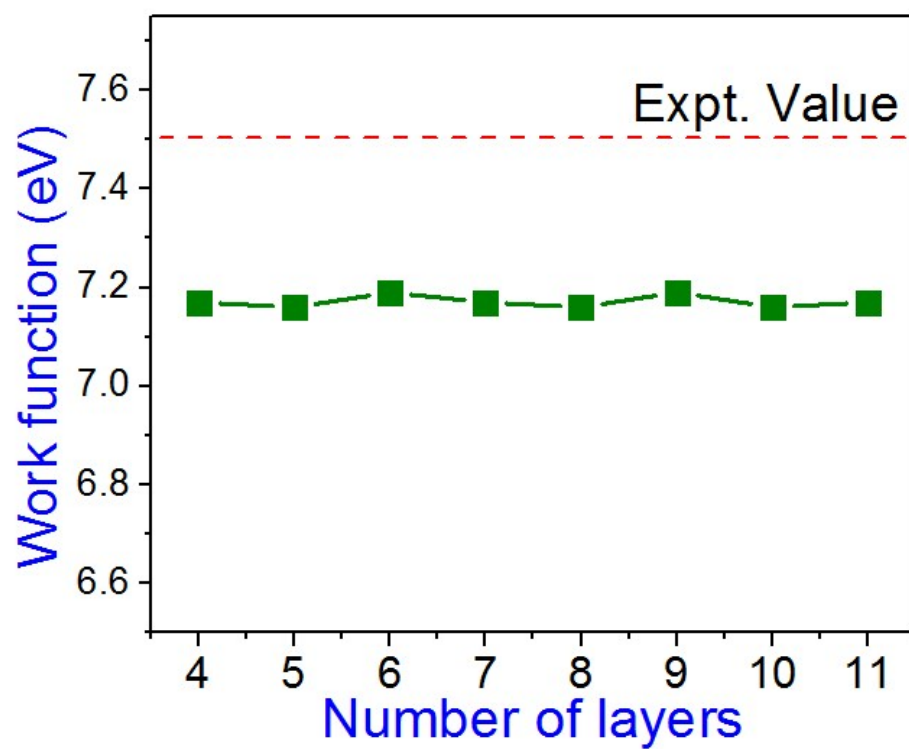
A standard three-electrode cell was used to measure the photoelectrochemical properties using potentiostat (VersaSTAT 4, Princeton Applied Research). A graphite and standard Ag/AgCl electrodes were used as counter and reference electrodes, respectively. For the working electrodes, 10 mg of sample powder was added to 10 ml of Liquion solution, which was subsequently sonicated for 1h and stirred overnight. The solution was then spin-coated onto a fluorine doped tin oxide (FTO) glass substrate and dried in an oven (60°C) overnight. 0.5 M Na<sub>2</sub>SO<sub>4</sub> solution as an electrolyte was prepared for the photoelectrochemical measurements. Xe lamp (300 W, 280 ~ 700 nm) was used to irradiate the working electrodes. Electrochemical impedance spectroscopy (EIS) was performed over the frequency range (0.01 ~ 10<sup>5</sup> Hz) under an AC applied voltage of 5 mV.

### ***Photocatalytic Hydrogen Evolution Analysis***

For sample preparation, 25 mg of photocatalysts were dispersed in 50 ml mixed aqueous

solution containing 0.35 M Na<sub>2</sub>S and 0.25 M Na<sub>2</sub>SO<sub>3</sub>. Nitrogen (N<sub>2</sub>) purging was conducted for the suspension during 30 min, which was then poured into a four-neck quartz reactor. Also, the reactor was sealed using a rubber septum and purged with argon (Ar) gas for 30 min. Xe lamp was positioned about 40 cm far from the sample where the radiant power was 73 mWcm<sup>-2</sup>. The produced gas was collected from the reactor using a syringe with 150 µL volume and injected into gas chromatography (6500GC, YL Instruments equipped with a thermal conductivity detector (TCD)) at 1 h intervals.

**- *Supporting Figures* -**



**FigureS1.** Computed work functions of anatase  $\text{TiO}_2(001)$  slab with varying thickness.

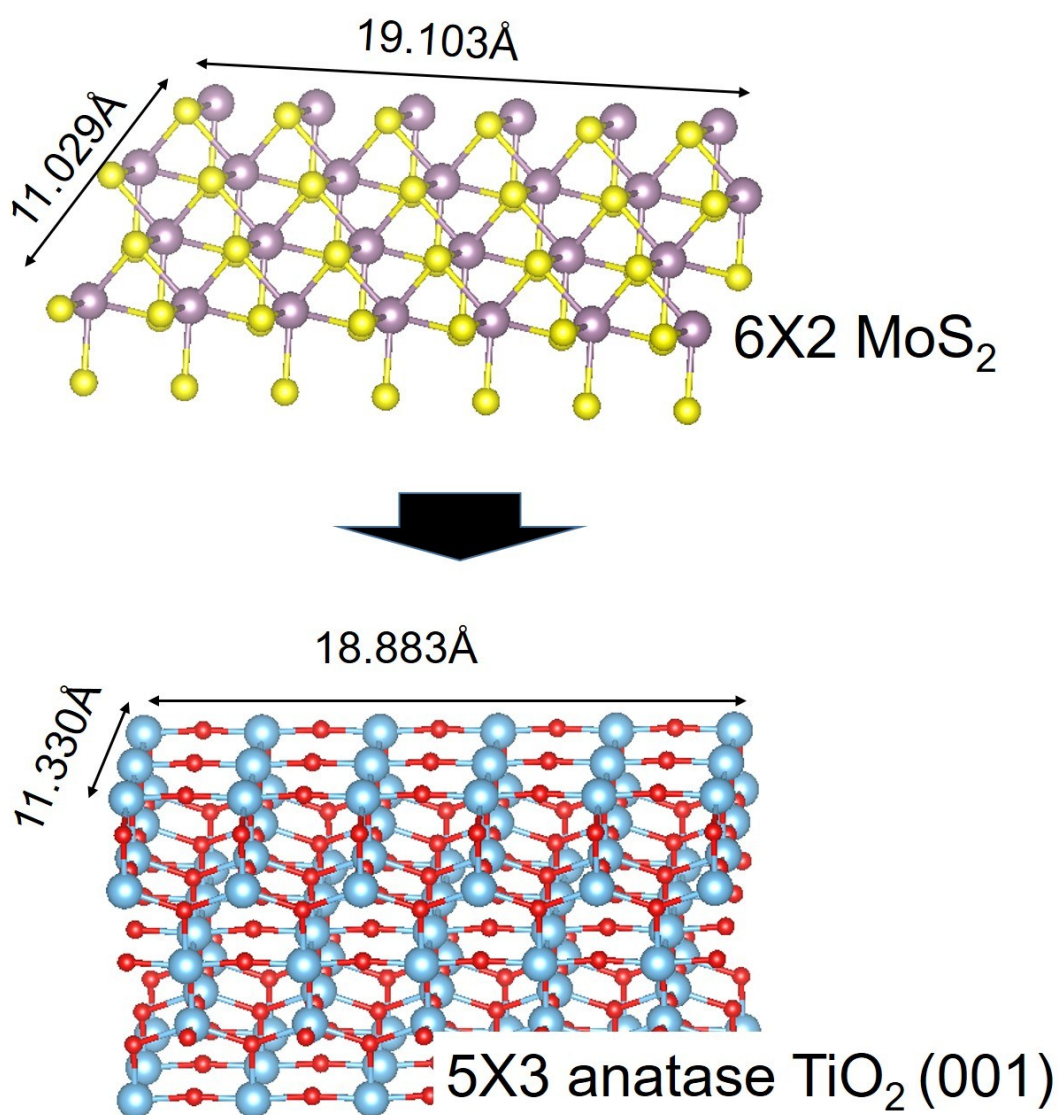


**Figure S2.** Supercell construction of 1T-MoS<sub>2</sub>/TiO<sub>2</sub>(001) junction. To fit the lateral dimension of the two materials, we used 6×2 ML-MoS<sub>2</sub> and 5×3 5ML-TiO<sub>2</sub>(001) slab. The purple, yellow, light blue, and red spheres are Mo, S, Ti, and O atoms.

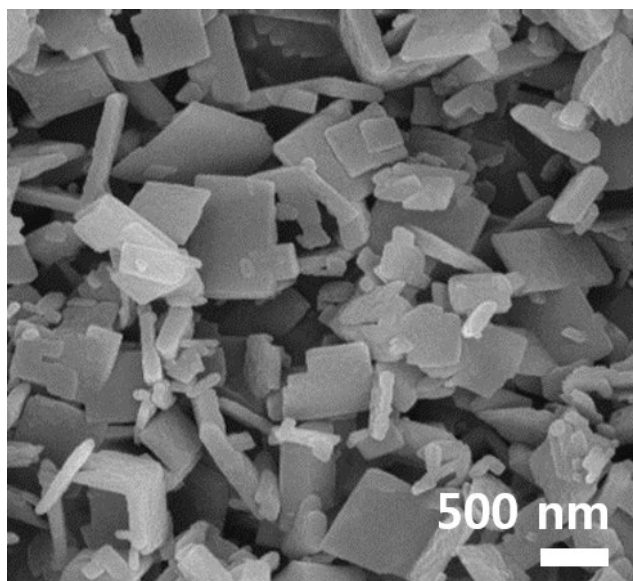


**Figure S3.** SEM image of 1T-MoS<sub>2</sub>/TiO<sub>2</sub>(001) nanocomposites.

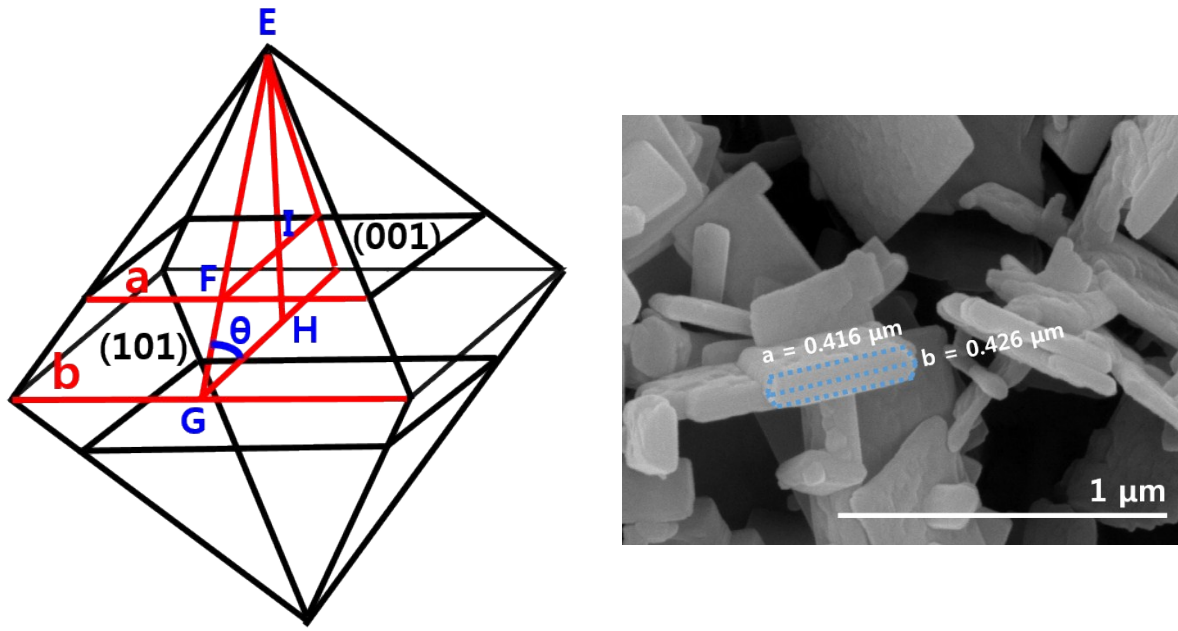


**Figure S4.** Slab model of anatase TiO<sub>2</sub> for calculating the proportion of (001) facet (left) and FE-SEM image of MST (right).

\*Calculation method of {001} facets percentage

$$S_{001} = 2a^2$$

$$S_{101} = 8(0.5EG \times b - 0.5EF \times a)$$

$$\begin{aligned} S_{001}\% &= \frac{S_{001}}{S_{001} + S_{101}} \\ &= \frac{2a^2}{2a^2 + 8(0.5EG \times b - 0.5EF \times a)} \\ &= \frac{a^2}{a^2 + 4(0.5 \times \frac{0.5b}{\cos\theta} \times b - 0.5 \times \frac{0.5a}{\cos\theta} \times a)} \\ &= \frac{a^2}{a^2 + \frac{b^2 - a^2}{\cos\theta}} = \frac{1}{\frac{b^2}{a^2} - 1} \\ &\quad \frac{1}{1 + \frac{a^2}{\cos\theta}} \end{aligned}$$

$$= \frac{\cos\theta}{\cos\theta + \frac{b^2}{a^2} - 1}$$

$\theta$  is equal to the theoretical value of  $68.3^\circ$  for the angle between the  $[001]$  and  $[101]$  facetes.

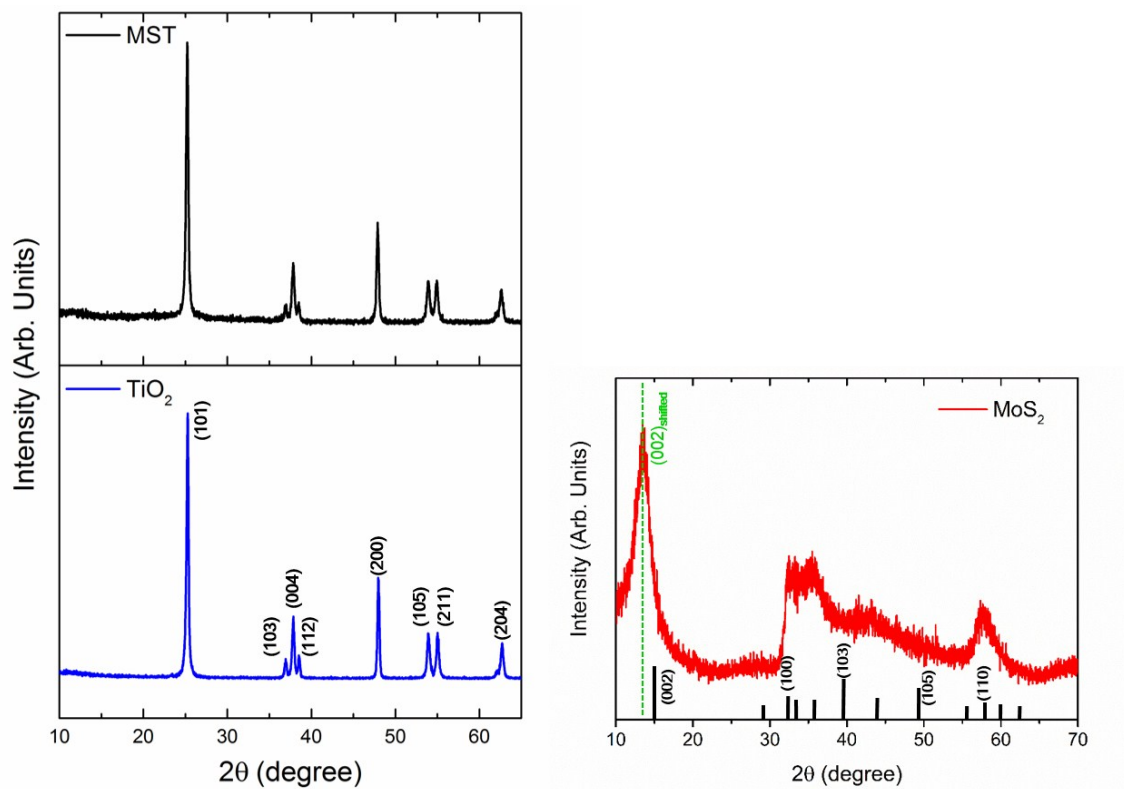


**Figure S5.** Powder X-ray patterns of pure  $\text{TiO}_2$ , MST, and  $\text{MoS}_2$  nanosheets.



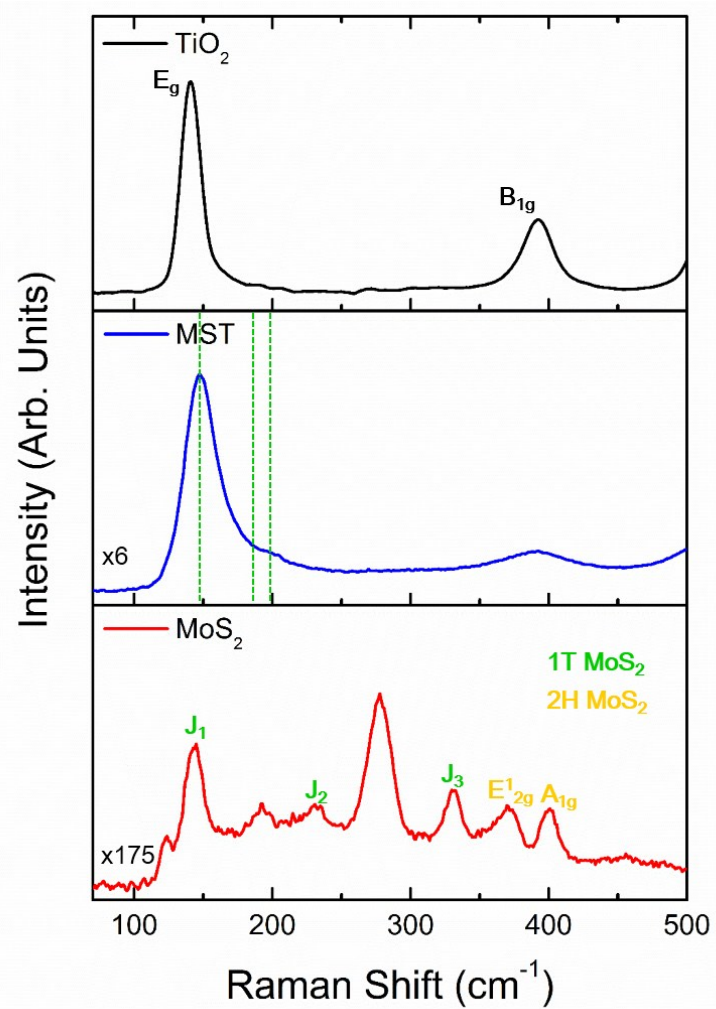


**Figure S6.** Raman spectra in the range of 100 ~ 500  $\text{cm}^{-1}$  of pure TiO<sub>2</sub>, MST and MoS<sub>2</sub> nanosheets.